The Proton's Weak Charge: γZ box contribution

Nathan Hall

CoEPP and CSSM,
University of Adelaide

P.G. Blunden, W. Melnitchouk, A.W. Thomas, R. D. Young

Adelaide-Jefferson Lab-Manitoba: "AJM"

Q_{weak}

- longitudinally polarised electrons scattering off fixed proton target.
- measures the proton's weak charge to within 4%.
- constrains New Physics at the $\sim$ TeV scale.
- measures the asymmetry:

$$A_{\text{PV}} = \frac{\sigma^+ - \sigma^-}{\sigma^+ + \sigma^-}$$

in the forward, elastic limit [Musolf *et al.*, Phys.Rep. 239:1],

$$A_{\text{PV}} = \frac{G_F}{4\pi\alpha\sqrt{2}}\, t\, Q_W^p$$

Q_{weak}

- longitudinally polarised electrons scattering off fixed proton target.
- measures the proton's weak charge to within 4%.
- constrains New Physics at the $\sim$ TeV scale.
- measures the asymmetry:

$$A_{\mathrm{PV}} = \frac{\sigma^+ - \sigma^-}{\sigma^+ + \sigma^-}$$

in the forward, elastic limit [Musolf *et al.*, Phys.Rep. 239:1],

$$A_{\mathrm{PV}} = \frac{G_F}{4\pi\alpha\sqrt{2}}\, t\, Q_W^p$$

proton's weak charge

Q_{weak}

At tree level,

$$Q_W^p = 1 - 4\sin^2\theta_W$$

For Q_{weak} precision aims, need to include radiative corrections also,
[Erler *et al.*, PRD 68:016006; 72:073003]

$$\begin{aligned} Q_W^p &= (1 + \Delta\rho + \Delta_e)\left(1 - 4\sin^2\theta_W(0) + \Delta_e^{'}\right) \\ &\quad + \Box_{WW} + \Box_{ZZ} + \Box_{\gamma Z}(0) \\ &= 0.0713 \pm 0.0008 \end{aligned}$$

- $\Delta\rho$ correction to the relative normalisation of the neutral and charged current amplitudes.
- Δ_e and $\Delta_e^{'}$ correction to axial-vector Zee and γee coupling.
- $\Box_{WW} \sim 26\%$ and $\Box_{ZZ} \sim 3\%$ (calculated perturbatively).

Q_{weak}

At tree level,

$$Q_W^p = 1 - 4\sin^2\theta_W$$

For Q_{weak} precision aims, need to include radiative corrections also,
[Erler *et al.*, PRD 68:016006; 72:073003]

$$\begin{aligned} Q_W^p &= (1 + \Delta\rho + \Delta_e)\left(1 - 4\sin^2\theta_W(0) + \Delta_e'\right) \\ &\quad + \Box_{WW} + \Box_{ZZ} + \Box_{\gamma Z}(0) \\ &= 0.0713 \pm 0.0008 \end{aligned}$$

- $\Delta\rho$ correction to the relative normalisation of the neutral and charged current amplitudes.
- Δ_e and Δ_e' correction to axial-vector Zee and γee coupling.
- $\Box_{WW} \sim 26\%$ and $\Box_{ZZ} \sim 3\%$ (calculated perturbatively).

Energy dependence of $\Box_{\gamma Z}$

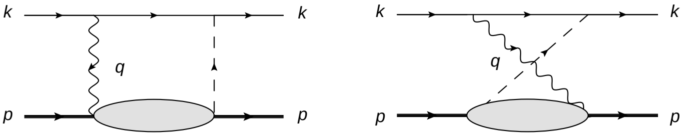

- contributions from both long and short distance physics
- decomposes into two parts,

$$\Box_{\gamma Z}(E) \;=\; \Box^{A}_{\gamma Z}(E) + \Box^{V}_{\gamma Z}(E)$$

Energy dependence of $\square_{\gamma Z}$

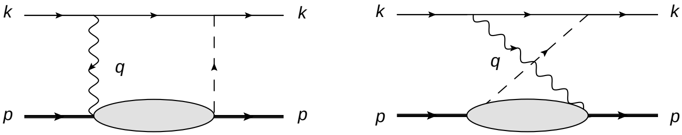

- contributions from both long and short distance physics

- decomposes into two parts,

$$\square_{\gamma Z}(E) \;=\; \boxed{\square^{A}_{\gamma Z}(E)} + \square^{V}_{\gamma Z}(E)$$

vector e – axial h

[Blunden *et al.*, PRL (2012)]

Energy dependence of $\Box_{\gamma Z}$

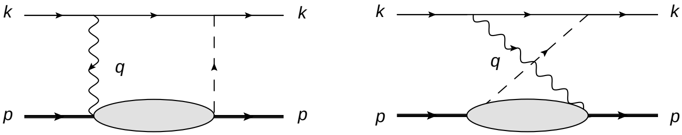

- contributions from both long and short distance physics
- decomposes into two parts,

$$\Box_{\gamma Z}(E) \;=\; \Box^{A}_{\gamma Z}(E) + \boxed{\Box^{V}_{\gamma Z}(E)}$$

axial e – vector h

Energy dependence of $\Box_{\gamma Z}^{V}$

$\Re e\, \Box_{\gamma Z}^{V}$ $(\times 10^{-3})$

time ↓

3 ± 3	Gorchtein and Horowitz, PRL (2009)
$4.7\,^{+1.1}_{-0.4}$	Sibirtsev *et al.* PRD (2010)
5.7 ± 0.9	Rislow and Carlson, PRD (2011)
5.4 ± 2.0	Gorchtein *et al.* PRC (2011)

$\Longrightarrow$ central values of all the calculations agree within the quoted uncertainties.

$\Longrightarrow$ error on the Gorchtein *et al.* value is twice as large as those on the Sibirtsev *et al.* and Rislow and Carlson calculations.

Energy dependence of $\Box_{\gamma Z}$

Summary list of the models for the γZ structure functions that have been discussed in the literature:

(i) color-dipole model, referred to as "Model I" in Gorchtein *et al.* (GHRM);

(ii) vector meson dominance (VMD) + Regge model, referred to as "Model II" by GHRM;

(iii) Sibirtsev *et al.*, based on the Regge parametrization of Capella *et al.* PLB (1994);

(iv) Rislow and Carlson's model: depends on the kinematic region.

Formalism

Dispersion relations give,

$$\Re e\,\Box^{V}_{\gamma Z}(E) \;=\; \frac{2E}{\pi}\mathcal{P}\int_0^{\infty} dE'\,\frac{1}{E'^2-E^2}\,\Im m\,\Box^{V}_{\gamma Z}(E')$$

From the optical theorem, the imaginary part of the PV γZ exchange amplitude can be written as [Gorchtein and Horowitz, PRL (2009)],

$$\Im m\,\Box^{V}_{\gamma Z}(E) \;=\; \frac{1}{(s-M^2)^2}\int_{W_\pi^2}^{s} dW^2\int_0^{Q^2_{\max}} dQ^2\,\frac{\alpha(Q^2)}{1+Q^2/M_Z^2} \times\left[F_1^{\gamma Z}+\frac{s\left(Q^2_{\max}-Q^2\right)}{Q^2\left(W^2-M^2+Q^2\right)}F_2^{\gamma Z}\right]$$

Formalism

Dispersion relations give,

$$\Re e \, \Box_{\gamma Z}^{V}(E) = \frac{2E}{\pi} \mathcal{P} \int_0^\infty dE' \frac{1}{E'^2 - E^2} \Im m \, \Box_{\gamma Z}^{V}(E')$$

From the optical theorem, the imaginary part of the PV γZ exchange amplitude can be written as [Gorchtein and Horowitz, PRL (2009)],

$$\Im m \, \Box_{\gamma Z}^{V}(E) = \frac{1}{(s - M^2)^2} \int_{W_\pi^2}^{s} dW^2 \int_0^{Q^2_{\max}} dQ^2 \, \frac{\alpha(Q^2)}{1 + Q^2/M_Z^2} \times \left[F_1^{\gamma Z} + \frac{s \left(Q^2_{\max} - Q^2 \right)}{Q^2 \left(W^2 - M^2 + Q^2 \right)} F_2^{\gamma Z} \right]$$

interference structure functions

Formalism

In describing the structure functions, or equivalently, the virtual boson–proton cross sections $\sigma_{T,L}$, it is convenient to separate the full range of kinematics into a resonance part and a smooth nonresonant background [Christy and Bosted, PRC (2010)],

$$\sigma_{T,L} \;=\; \sigma_{T,L}^{(\mathrm{res})} + \sigma_{T,L}^{(\mathrm{bgd})}$$

$\sigma_{T,L}^{(\mathrm{res})}$
$\Longrightarrow$ term includes a sum over the prominent low-lying resonances.

$\sigma_{T,L}^{(\mathrm{bgd})}$
$\Longrightarrow$ is determined phenomenologically by fitting the inclusive scattering data.

γZ structure functions - resonances

◦ Using isospin symmetry, the matrix elements of the vector component of the Z current for a proton target can be related to the proton and neutron matrix elements of the electromagnetic current by

$$\langle R| J_Z^\mu |p\rangle \;\; = \;\; (1 - 4\sin^2\theta_W)\langle R| J_\gamma^\mu |p\rangle \; - \; \langle R| J_\gamma^\mu |n\rangle$$

$\Longrightarrow$ neglecting the small contribution from strange quarks.

◦ Modify the contribution from each resonance R by a ratio that takes into account the differences between the electromagnetic and weak neutral transition amplitudes.

γZ structure functions - resonances

For the transverse cross section define this ratio for a proton as

$$\xi_R \equiv \frac{\sigma^{\gamma Z}_{T,R}}{\sigma^{\gamma\gamma}_{T,R}} = (1 - 4\sin^2\theta_W) - y_R$$

where,

$$y_R = \frac{A^{p}_{R,\frac{1}{2}} A^{n^*}_{R,\frac{1}{2}} + A^{p}_{R,\frac{3}{2}} A^{n^*}_{R,\frac{3}{2}}}{\left|A^{p}_{R,\frac{1}{2}}\right|^2 + \left|A^{p}_{R,\frac{3}{2}}\right|^2}$$

$\Longrightarrow$ GHRM longitudinal ratio equated with the transverse one.

$\Longrightarrow$ no Q^2 dependence (errors large enough to take this into account).

γZ structure functions - background

For Model II of GHRM, a generalization of the VMD model is used, assuming the γZ cross section for vector meson V is given by the analogous $\gamma\gamma$ cross section scaled by the ratio κ_V of weak and electric charges,

$$\sigma_{T,L}^{\gamma Z(V)} = \kappa_V \, \sigma_{T,L}^{\gamma\gamma(V)}$$

where,

$$\kappa_\rho = 2 - 4\sin^2\theta_W \quad \kappa_\omega = -4\sin^2\theta_W \quad \kappa_\phi = 3 - 4\sin^2\theta_W$$

This allows the ratio of γZ to $\gamma\gamma$ cross sections to be written as

$$\frac{\sigma_{T,L}^{\gamma Z}}{\sigma_{T,L}^{\gamma\gamma}} = \frac{\kappa_\rho + \kappa_\omega \, R_\omega^{T,L}(Q^2) + \kappa_\phi \, R_\phi^{T,L}(Q^2) + \kappa_C^{T,L} \, R_C^{T,L}(Q^2)}{1 + R_\omega^{T,L}(Q^2) + R_\phi^{T,L}(Q^2) + R_C^{T,L}(Q^2)}$$

γZ structure functions - background

For Model II of GHRM, a generalization of the VMD model is used, assuming the γZ cross section for vector meson V is given by the analogous $\gamma\gamma$ cross section scaled by the ratio κ_V of weak and electric charges,

$$\sigma_{T,L}^{\gamma Z(V)} = \kappa_V \, \sigma_{T,L}^{\gamma\gamma(V)}$$

where,

$$\kappa_\rho = 2 - 4\sin^2\theta_W \quad \kappa_\omega = -4\sin^2\theta_W \quad \kappa_\phi = 3 - 4\sin^2\theta_W$$

This allows the ratio of γZ to $\gamma\gamma$ cross sections to be written as

$$\frac{\sigma_{T,L}^{\gamma Z}}{\sigma_{T,L}^{\gamma\gamma}} = \frac{\kappa_\rho + \kappa_\omega \, R_\omega^{T,L}(Q^2) + \kappa_\phi \, R_\phi^{T,L}(Q^2) + \kappa_C^{T,L} \, R_C^{T,L}(Q^2)}{1 + R_\omega^{T,L}(Q^2) + R_\phi^{T,L}(Q^2) + R_C^{T,L}(Q^2)}$$

AJM model - $F_i^{\gamma\gamma}$

Divide the integrals into distinct regions of W^2 and Q^2,

(I) Christy and Bosted's (CB) parametrization [Christy and Bosted PRC (2010)] to describe the low-W region (Region I) at $W_\pi < W < 2$ GeV for all Q^2 up to 10 GeV^2;

(II) At higher W, corresponding to kinematics where Regge theory is applicable, the VMD+Regge model of Alwall and Ingelman [Alwall and Ingleman, PLB (2004)] is combined with a modified CB resonance contribution to describe the structure functions for $W^2 > 9$ GeV^2 and $Q^2 < 2.5$ GeV^2;

(III) In the DIS region we use the next-to-next-to-leading order (NNLO) fit by Alekhin *et al.* (ABM11) [Alekhin *et al.*, PRD (2012)].

AJM model - $F_i^{\gamma\gamma}$

Kinematic regions:

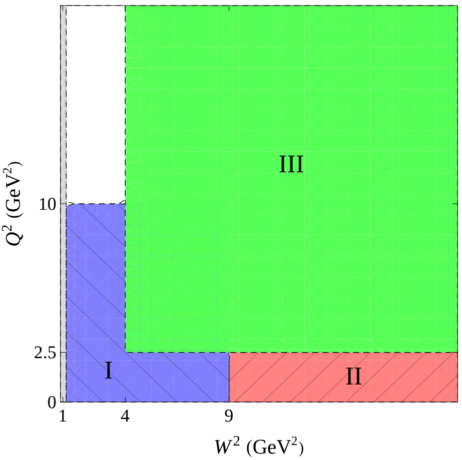

AJM model - $F_i^{\gamma Z}$

Resonances: modified using the ratio ξ_R,

$$\xi_R \equiv \frac{\sigma_{T,R}^{\gamma Z}}{\sigma_{T,R}^{\gamma\gamma}} = (1 - 4\sin^2\theta_W) - y_R$$

where

$$y_R = \frac{A^p_{R,\frac{1}{2}} A^{n^*}_{R,\frac{1}{2}} + A^p_{R,\frac{3}{2}} A^{n^*}_{R,\frac{3}{2}}}{\left|A^p_{R,\frac{1}{2}}\right|^2 + \left|A^p_{R,\frac{3}{2}}\right|^2}$$

as in GHRM.

- for the AJM model the uncertainties of the helicity amplitudes are added quadrature, while GHRM take the extremal values for each resonance.

AJM model - $F_i^{\gamma Z}$

Nonresonant background: transformed using,

$$\frac{\sigma^{\gamma Z}_{T,L}}{\sigma^{\gamma\gamma}_{T,L}} = \frac{\kappa_\rho + \kappa_\omega\, R_\omega^{T,L}(Q^2) + \kappa_\phi\, R_\phi^{T,L}(Q^2) + \kappa_C^{T,L}\, R_C^{T,L}(Q^2)}{1 + R_\omega^{T,L}(Q^2) + R_\phi^{T,L}(Q^2) + R_C^{T,L}(Q^2)}$$

- instead of fixing the parameters $\kappa_C^{T,L}$, determine by demanding that structure functions match at their boundaries.

DIS region: computed from the ABM11 PDF parametrization [Alekhin *et al.*, PRD 86:054009].

PDF constraints

Our fit of the parameters $\kappa_C^{T,L}$ involves equating the cross section ratios $\sigma_{T,L}^{\gamma Z}/\sigma_{T,L}^{\gamma\gamma}$ with the structure function ratios computed from global QCD fits in the DIS region,

$$\frac{\sigma_T^{\gamma Z}}{\sigma_T^{\gamma\gamma}} = \left.\frac{F_1^{\gamma Z}}{F_1^{\gamma\gamma}}\right|_{\rm DIS} \qquad \frac{\sigma_L^{\gamma Z}}{\sigma_L^{\gamma\gamma}} = \left.\frac{F_L^{\gamma Z}}{F_L^{\gamma\gamma}}\right|_{\rm DIS}$$

$\Longrightarrow$ DIS structure functions $F_{1,L}^{\gamma\gamma,\gamma Z}$ are taken from the ABM11 parametrization.

$\Longrightarrow$ determine the values of $\kappa_C^{T,L}$ by matching the ratios, over a range of W^2 values at fixed Q^2 near the boundaries between the regions.

PDF constraints

Our fit of the parameters $\kappa_C^{T,L}$ involves equating the cross section ratios $\sigma^{\gamma Z}_{T,L}/\sigma^{\gamma\gamma}_{T,L}$ with the structure function ratios computed from global QCD fits in the DIS region,

$$\frac{\sigma_T^{\gamma Z}}{\sigma_T^{\gamma\gamma}} = \left.\frac{F_1^{\gamma Z}}{F_1^{\gamma\gamma}}\right|_{\mathrm{DIS}} \qquad \frac{\sigma_L^{\gamma Z}}{\sigma_L^{\gamma\gamma}} = \left.\frac{F_L^{\gamma Z}}{F_L^{\gamma\gamma}}\right|_{\mathrm{DIS}}$$

$\Longrightarrow$ DIS structure functions $F_{1,L}^{\gamma\gamma,\gamma Z}$ are taken from the ABM11 parametrization.

$\Longrightarrow$ determine the values of $\kappa_C^{T,L}$ by matching the ratios, over a range of W^2 values at fixed Q^2 near the boundaries between the regions.

PDF constraints

Values at the different Q^2 are correlated

$\Longrightarrow$ performing a simple χ^2 fit will underestimate the errors.

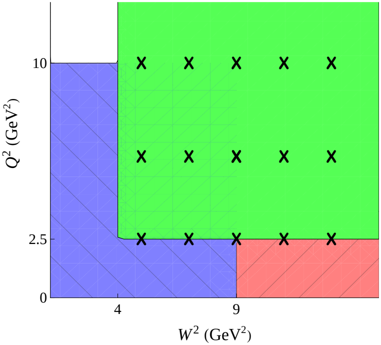

Uncertainties come from:

(i) the W^2 dependence;

(ii) the PDF error.

PDF constraints

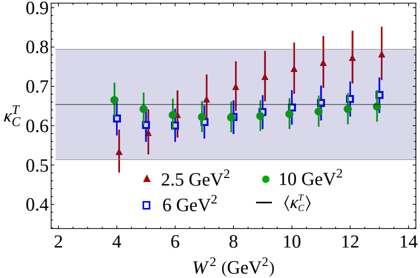

$$\Longrightarrow \kappa_C^T = 0.65 \pm 0.14$$

$$\kappa_C^L = -1.3 \pm 1.7 \Longleftarrow$$

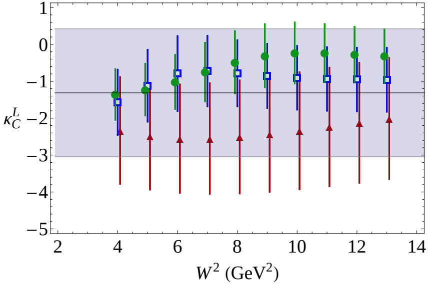

AJM model - $F_2^{\gamma Z}$

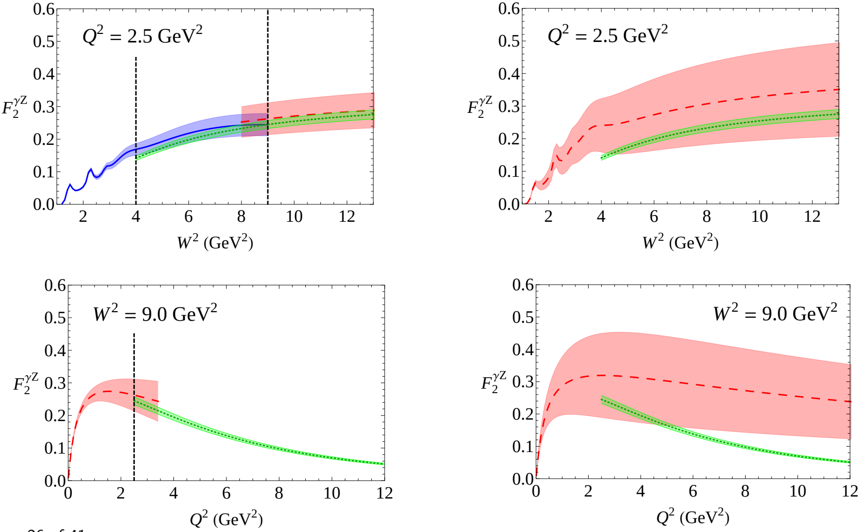

PVDIS asymmetry

May perform a proof of method using the parity-violating inelastic asymmetry data for the deuteron [Wang *et al*. PRL 111, 082501],

$$A_{\mathrm{PVDIS}} = g_A^e \left(\frac{G_F Q^2}{2\sqrt{2}\pi\alpha} \right) \times \frac{xy^2 F_1^{\gamma Z} + \left(1 - y - \frac{x^2 y^2 M^2}{Q^2}\right) F_2^{\gamma Z} + \frac{g_V^e}{g_A^e}\left(y - \frac{1}{2}y^2\right) x F_3^{\gamma Z}}{xy^2 F_1^{\gamma\gamma} + \left(1 - y - \frac{x^2 y^2 M^2}{Q^2}\right) F_2^{\gamma\gamma}}$$

Deuteron asymmetry

◦ Measured parity-violating asymmetry A^{d}_{PV} [Wang *et al.* PRL 111, 082501], scaled by $1/Q^2$, is shown at $W = 1.26$, 1.59, 1.86 and 1.98 GeV, with Q^2 values ranging from 0.76 GeV^2 to 1.47 GeV^2 (preliminary).

◦ Deuteron asymmetries in the AJM model are computed with the continuum parameters constrained by the DIS region structure functions, as for the proton asymmetry.

◦ Resulting fit gives,

$$\kappa_C^T(d) = 0.79 \pm 0.05 \qquad \kappa_C^L(d) = 0.2 \pm 3.4$$

Deuteron asymmetry

PDF constrained:

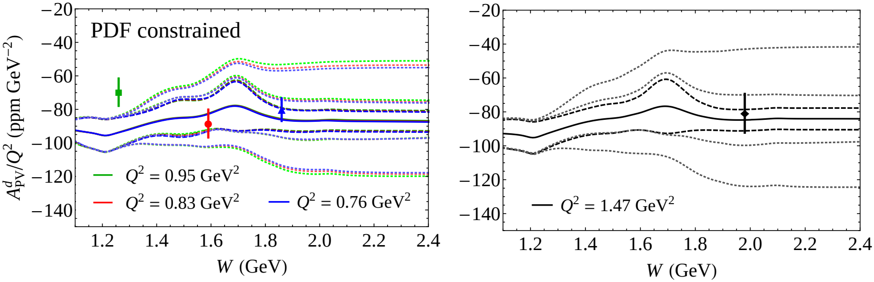

$\Longrightarrow$ clearly in good agreement with the E08-011 [Wang *et al.* PRL 111, 082501] data.

Deuteron Asymmetry

Data constrained:

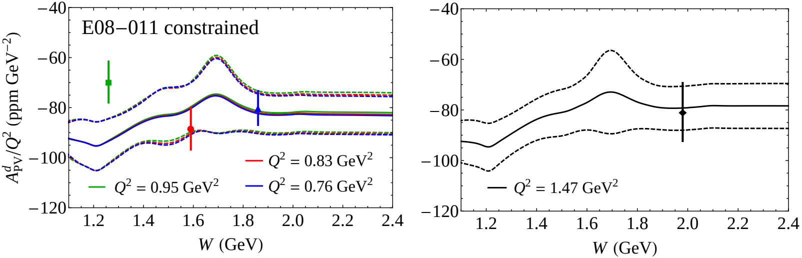

This fit constrains $\kappa_C^T(d) = 0.69 \pm 0.13$.

Energy dependence of $\Re e \,\Box_{\gamma Z}^{V}$

Dependence of $\Re e \,\Box_{\gamma Z}^{V}$ on the incident energy E:

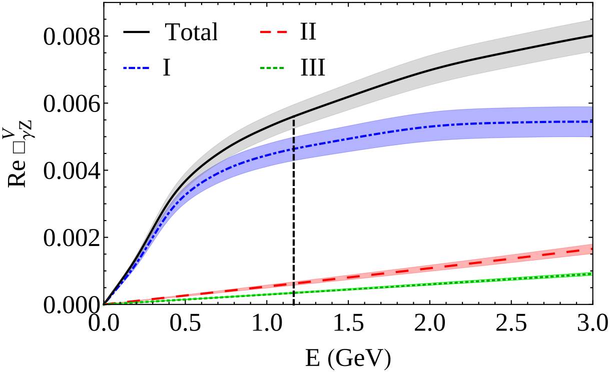

[Hall *et al.* PRD (2013)]

$\Re e\,\Box_{\gamma Z}^{V}$ at Q_{weak}

Region	$\Re e\,\Box_{\gamma Z}^{V}$ $(\times 10^{-3})$
I (res)	2.18 ± 0.29
I (bgd)	2.46 ± 0.21
I (total)	4.64 ± 0.36
II	0.59 ± 0.05
III	0.35 ± 0.02
Total	5.57 ± 0.36

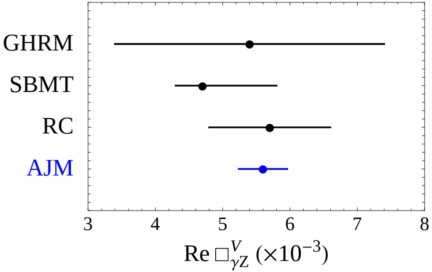

Including all uncertainties, we find for the total correction

$$\Re e\,\Box_{\gamma Z}^{V} = (5.57 \pm 0.21_{[bgd]} \pm 0.29_{[res]} \pm 0.02_{[DIS]}) \times 10^{-3}$$

Adding the errors in quadrature gives

$$\Re e\,\Box_{\gamma Z}^{V} = (5.57 \pm 0.36) \times 10^{-3}$$

Conclusions

• We have performed a comprehensive analysis of the γZ box contribution to the forward, *e–p* elastic parity-violating asymmetry, reporting a final value of

$$\Re e\,\Box_{\gamma Z}^{V} = (5.57 \pm 0.36) \times 10^{-3}.$$

• The reduction of the error, relative to previous works, is largely driven by data, where theoretical uncertainties are constrained by a consistent description of the γZ interference structure functions.

• May also use this method to determine the $\Re e\,\Box_{\gamma Z}^{V}$ contribution at higher energies relevant to MOLLER, reporting a value of $\Re e\,\Box_{\gamma Z}^{V} = (11.5 \pm 0.8) \times 10^{-3}$ [Hall *et al.* PLB (2014)]

• Important to further examine the Q^2 dependence of the $\Re e\,\Box_{\gamma Z}^{V}$

Deuteron asymmetry – unbinned

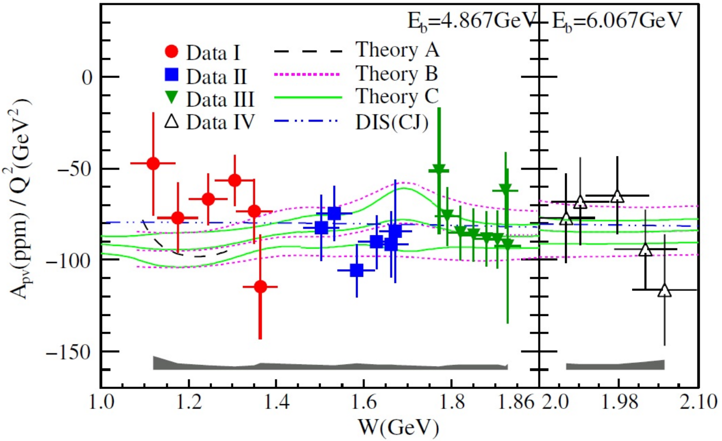

[Wang *et al.*, PRL (2013)]

Christy-Bosted fit

[Christy and Bosted, PRC 81:055213]

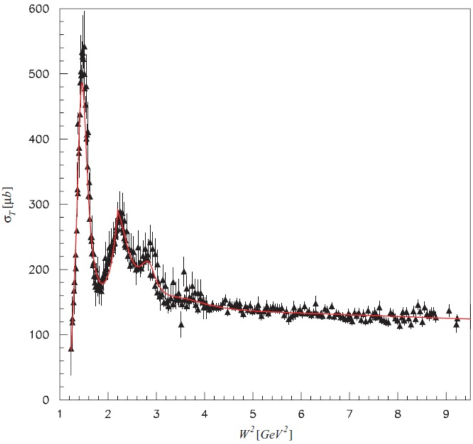

MOLLER

- longitudinally polarised electrons scattered off atomic electrons in a liquid hydrogen target.
- measure the electron's weak charge to within 2.3%.
  $\Longrightarrow$ equivalent to measuring $\sin^2\theta_W$ to $\approx 0.1\%$.
- PV asymmetry is given by [Derman and Marciano, Annals Phys. 121:147]:

$$A_{\rm PV} \quad = \quad m_e E \, \frac{G_F}{\sqrt{2}\pi\alpha} \frac{2y(1-y)}{1+y^4+(1-y)^4} \, Q_W^e$$

where at tree level,

$$Q_W^e = -1 + 4\sin^2\theta_W$$

Experimental status of $\sin^2\theta_W$

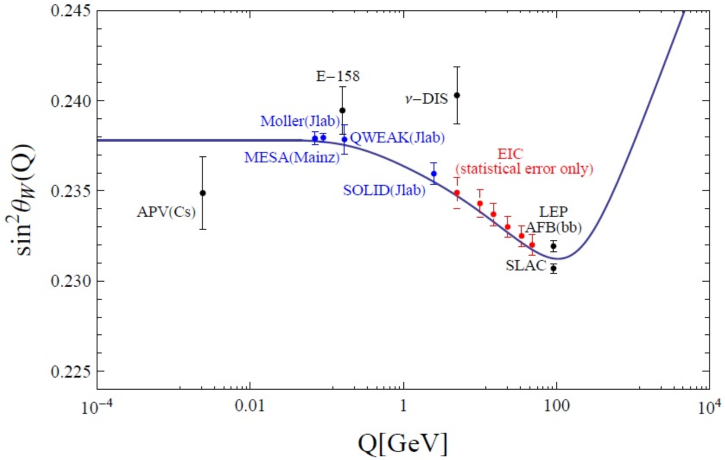

[Kumar *et al.*, Ann. Rev. Nucl. Part. Sci. (2013)]

MOLLER backgrounds

Use of hydrogen target means unavoidable background contribution from $e - p$ scattering.

Require,

(I) $Q_W^p < 4\%$ level

(II) proton inelastic asymmetry $\sim 10\%$

$$A_{\rm PVDIS} = g_A^e \left(\frac{G_F Q^2}{2\sqrt{2}\pi\alpha}\right) \times \frac{xy^2 F_1^{\gamma Z} + \left(1 - y - \frac{x^2 y^2 M^2}{Q^2}\right) F_2^{\gamma Z} + \frac{g_V^e}{g_A^e}\left(y - \frac{1}{2}y^2\right) x F_3^{\gamma Z}}{xy^2 F_1^{\gamma\gamma} + \left(1 - y - \frac{x^2 y^2 M^2}{Q^2}\right) F_2^{\gamma\gamma}}$$

$\Re e\,\Box^V_{\gamma Z}$ at MOLLER

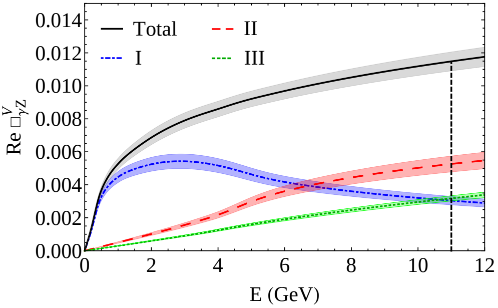

Dependence of $\Re e\,\Box^V_{\gamma Z}$ on the incident energy E.

Region	$\Re e\,\Box^V_{\gamma Z}$ $(\times 10^{-3})$	
	Q_{weak}	MOLLER
I	4.64 ± 0.35	3.04 ± 0.26
II	0.59 ± 0.05	5.26 ± 0.49
III	0.35 ± 0.02	3.18 ± 0.16
total	5.57 ± 0.36	11.5 ± 0.6

Model dependence of Reg II

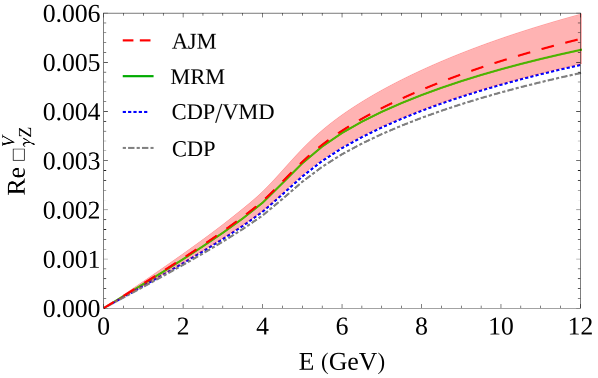

$\Longrightarrow$ including all uncertainties, we find for the total correction

$$\Re e\, \Box^V_{\gamma Z} = (11.5 \pm 0.6_{\,\mathrm{orig}} \pm 0.6_{\,\mathrm{mdp}}) \times 10^{-3}$$

Inelastic asymmetry at 11 GeV

A_{PVDIS} background to MOLLER